Electroluminescence of Bisindolylmaleimide Derivatives Containing Pentafluorophenyl Substituents

Tzu-San Yeh,[†] Tahsin J. Chow,*[,‡] Sheng-Heng Tsai,[‡] Ching-Wen Chiu,[‡] and Cheng-Xue Zhao*[,§]

Institute of Chemistry, Academia Sinica, Taipei, 115 Taiwan, ROC, Department of Chemistry, National Changhua University of Education, Changhua, 500 Taiwan, ROC, and Department of Chemistry, Shanghai Jiaotong University, Shanghai 200240, China

Received October 4, 2005. Revised Manuscript Received November 30, 2005

Bisindolylmaleimide derivatives containing nonfluorinated (**1**−**3**) and fluorinated (**1F**−**4F**) substituents were synthesized, and their performances on electroluminescence devices were compared. Two kinds of devices were fabricated, in which either AlQ_3 (tris(8-hydroxyquinolinato)aluminum) or TPBI (2,2′,2″-(1,3,5-benzenetriyl)tris(1-phenyl-1*H*-benzimidazole)) was used as an electron-transporting (ET) medium. For nonfluorinated materials **1**−**3**, a red emission was obtained in devices with an ITO/NPB/**1**−**3**/TPBI/Mg:Ag configuration (ITO and NPB denote indium−tin oxide and 4,4′-bis[*N*-(1-naphthyl)-*N*-phenylamino]-biphenyl, respectively), whereas dual emissions were observed in others using AlQ_3 as the ET material. For fluorinated materials **1F**−**4F**, dual emissions were observed in both kinds of devices. The second emission came from the ET layer, although a certain number of holes were annihilated with the electrons there. Compounds bearing pentafluorophenyl moieties exhibited a reduced potential energy for both the HOMO and LUMO levels and thus lowered the barrier for the hole moving across the film interface. Typical devices with an ITO/NPB/dye/TPBI/Mg:Ag configuration exhibited a red to purple color, which showed turn-on voltages of ∼4 V, a maximum luminescence of 2700−5400 Cd/m^2 at 14 V, and an external quantum efficiency of 0.3−0.6%. Devices with an ITO/NPB/dye/AlQ_3/Mg:Ag configuration exhibited a yellow to green color, which showed turn-on voltages of ∼4 V, a maximum luminescence of 7000−16000 Cd/m^2 at 13 V, and an external quantum efficiency of 0.4−0.7%.

Introduction

Bisindolylmaleimides are derivatives of Arcyriarubins A (**6**), which belongs to a family of pigments produced by the slime molds (*Myxomycetes*).[1] In our previous reports,[2] we effectively used these compounds as red luminescence materials in the fabrication of light-emitting diodes (LED).[3] Organic materials that exhibit red luminescence are usually highly polar molecules.[4−6] They tend to form microcrystals in the solid state and self-quench their luminescence. The most unique feature of bisindolylmaleimides is the persistence of red emissions even in the solid state. Our previous study showed that these groups of compounds form amorphous glasses because of the conformational flexibility of both indolyl moieties.[2] The substituents at C(2′) of the indoles repel each other, thereby twisting the molecules away from a planar geometry.

During the analyses of electroluminescence devices, we observed some intriguing effects when the *N*-phenyl substituents were replaced by pentafluorophenyl groups, such as **1F** and **4F**. The charge mobility in the solid medium of the material containing pentafluorophenyl groups seems to be higher than in those without fluorine substituents. The high electronegativity of the fluorine atoms was known to reduce the potential energy of high-lying molecular orbitals.[7] For instance, it has been shown that perfluorophenyl substituents can effectively promote the charge mobility and thermal stability of thin-film transistors (TFT).[8] Fluorine substituents may have several other potential advantages, such as enhancing emission efficiency, minimizing self-

* To whom correspondence should be addressed. Fax: (886)-2-27884179. E-mail: tjchow@chem.sinica.edu.tw.
† National Changhua University of Education.
‡ Academia Sinica.
§ Shanghai Jiaotong University.

(1) Steglich, W.; Steffan, B.; Kopanski, L.; Eckhardt, G. *Angew. Chem.* **1980**, *92*, 463; *Angew. Chem., Int. Ed.* **1980**, *19*, 459.
(2) Chiu, C.-W.; Chow, T. J.; Chuen, C.-H.; Lin, H.-M.; Tao, Y.-T. *Chem. Mater.* **2003**, *15*, 4527−4532.
(3) (a) *Handbook of Luminescence Display Materials & Devices, Vol. 1: Organic Light-Emitting Diodes*; Nalwa, H. S., Rohwer, L. S., Eds.; American Scientific Publishers: Stevenson Ranch, CA, 2003. (b) Mitsche, U.; Bauerle, P. *J. Mater. Chem.* **2000**, *10*, 1471−1507.
(4) (a) Okada, K.; Wang, Y.-F.; Chen, T.-M.; Kitamura, M.; Nakaya, T.; Inoue, H. *J. Mater. Chem.* **1999**, *9*, 3023. (b) Kido, J.; Endo, J. *Chem. Lett.* **1997**, 633. (c) Picciolo, L. C.; Murata, H.; Kafafi, Z. H. *Appl. Phys. Lett.* **2001**, *78*, 2378.
(5) (a) Thomas, K. R. J.; Lin, J. T.; Tao, Y. T.; Chuen, C.-H. *Adv. Mater.* **2002**, *14*, 822. (b) Wu, W.-C.; Yeh, H.-C.; Chan, L.-H.; Chen, C.-T. *Adv. Mater.* **2002**, *14*, 1072. (c) Tang, C. W.; Van Slyke, S. A.; Chen, C. H. *J. Appl. Phys.* **1989**, *65*, 3610.
(6) (a) Bulovic, V.; Shoustikov, A.; Baldo, M. A.; Bose, E.; Kozlov, V. G.; Thompson, M. E.; Forrest, S. R. *Chem. Phys. Lett.* **1998**, *287*, 455. (b) Tao, X. T.; Miyata, S.; Sasabe, H.; Zhang, G. J.; Wada, T.; Jiang, M. H. *Appl. Phys. Lett.* **2001**, *78*, 279.
(7) (a) Chen, H.-Z.; Shi, M.-M.; Aernouts, T.; Wang, M.; Borghs, G.; Heremans, P. *Sol. Energy Mater. Sol. Cells* **2005**, *87*, 521−527. (b) Irie, M. *Chem. Rev.* **2000**, *100*, 1685−1716. (c) Matsui, M.; Shibata, K.; Muramatsu, H.; Sawada, H.; Nakayama, M. *Chem. Ber.* **1992**, *125*, 467−471.
(8) (a) Facchetti, A.; Yoon, M.-H.; Stern, C. L.; Katz, H. E.; Marks, T. J. *Angew. Chem., Int. Ed.* **2003**, *42*, 3900−3903. (b) Newman, C. R.; Frisbie, C. D.; da Silva Filho, D. A.; Bre'das, J.-L.; Ewbank, P. C.; Mann, K. R. *Chem. Mater.* **2004**, *16*, 4436−4451.

10.1021/cm052198y CCC: $33.50
Published on Web 01/10/2006

quenching, and improving the film morphology of materials.[9] To understand the property of perfluorophenyl groups, we prepared a series of maleimides containing both pentafluorophenyl and pentafluorobenzyl substituents. The physical properties of compound pairs **1**/**1F**, **2**/**2F**, and **3**/**3F** were analyzed, and their performances on LED devices were compared.

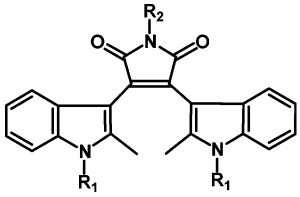

1) $R_1 = CH_3$; $R_2 = C_6H_5$
1F) $R_1 = CH_3$; $R_2 = C_6F_5$
2) $R_1 = CH_3$; $R_2 = CH_2C_6H_5$
2F) $R_1 = CH_3$; $R_2 = CH_2C_6F_5$
3) $R_1 = R_2 = CH_2C_6H_5$
3F) $R_1 = R_2 = CH_2C_6F_5$

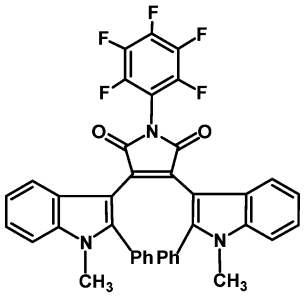

4F

Experimental Section

Instrumentation. Absorption spectra were taken on a Hewlett-Packard 8453 spectrophotometer and emission spectra on a Hitachi F-4500 fluorescence spectrophotometer. Infrared spectra were taken on a Perkin-Elmer L118-F000 FT-IR spectrometer. ^{1}H, ^{13}C, and ^{19}F NMR spectra were recorded on Bruker AC300, AV400, AV500, and AMX400 superconducting FT NMR spectrometers. The signal of tetramethylsilane at δ 0.00 was used as an internal standard for both ^{1}H and ^{13}C NMR spectra, whereas that of trichlorofluoromethane was used for ^{19}F. Mass spectra were taken on a Joel JMS 700 double-focusing spectrometer, facilitated with fast atom bombardment (FAB) for sample ionization. Microanalyses were completed on a Perkin-Elmer 2400 elemental analyzer. Melting points of the compounds were uncorrected. X-ray diffraction analyses were done on a Bruker AXS SMART-1000 spectrometer. Differential scanning calorimetry was done on a Perkin-Elmer DCS-7 instrument. Cyclic voltammetry measurements were carried out on a BAS 100B electrochemical analyzer equipped with a conventional three-electrode system, i.e., glassy carbon, platinum wire, and $Ag/AgNO_3$ as the working, counter, and reference electrodes, respectively. Degassed acetonitrile solution with 0.1 M tetra-*n*-butylammonium hexafluorophosphate was used as the electrolyte. E_{ox} and E_{red} data were measured with reference to a ferrocene (Fc) internal standard that was calibrated to +350 mV against a $Ag/AgNO_3$ reference electrode. Measurements were taken at a scan rate of 100 mV s^{-1}.

Device Fabrication. Indium−tin oxide (ITO)-coated glass with a sheet resistance of <50 Ω was used as the substrate. The substrate was prepatterned by photolithography, giving an effective device size of 3.14 mm^2. Pretreatment of ITO includes a routine chemical cleaning using detergent and alcohol in sequence, followed by oxygen plasma cleaning. Thermal evaporation of organic materials was carried out using ULVAC Cryogenics at a chamber pressure of 10^{-6} Torr. Two types of devices were configured with ITO/NPB (40 nm)/maleimide (10 nm)/AlQ_3 (40 nm)/Mg:Ag (device A) and ITO/NPB (40 nm)/maleimide (10 nm)/TPBI (40 nm)/Mg:Ag (device B) formats, in which NPB, AlQ_3, and TPBI are 4,4′-bis-[*N*-(1-naphthyl)-*N*-phenylamino]biphenyl, tris(8-hydoxyquinolinato)aluminum, and 2,2′,2″-(1,3,5-benzenetriyl)tris(1-phenyl-1*H*-benzimidazole), respectively. Mg and Ag were coevaporated into a $Mg_{0.9}Ag_{0.1}$ (50 nm) alloy, which was then capped by a thick layer of silver and used as the cathode. Current-voltage and light-intensity measurements were done on a Keithley 2400 source meter and a Newport 1835C optical meter equipped with a Newport 818-ST silicon photodiode, respectively. All measurements were completed under ambient conditions.

2,3-Bis(2′,*N*-dimethyl-3′-indolyl)-*N*-phenylmaleimide (1). To a toluene (150 mL) solution of 2-methylindole (5.0 g, 38 mmol) was added MeMgCl (3 M in THF, 15.2 mL) at room temperature under a nitrogen atmosphere, and the solution was heated to 60 °C for 1 h. A solution of dibromomaleimide (1.94 g, 7.7 mmol) in toluene (20 mL) was then added to the solution, which was heated to reflux for 24 h. The solution turned from red to dark blue. It was cooled to room temperature and diluted with ethyl acetate (250 mL). The combined organic part was successively washed with HCl (1.0 N, 100 mL), water (100 mL), and brine (100 mL); it was then dehydrated over anhydrous $MgSO_4$. It was dried in vacuo, forming a dark red residue. The crude product was purified by silica gel column chromatography with ethyl acetate/hexane (1:1) as the eluant, affording bis-2-methylindolylmaleimide (**6**) (2.4 g, 88% yield).

To an aqueous solution (50 mL) of 10% KOH was added an ethanol solution (20 mL) of **6** (2.0 g, 5.6 mmol). The mixture was heated to reflux for 24 h and then neutralized by the addition of hydrochloric acid (2 N) until precipitates formed. It was filtered, and the filtrates were dried in vacuo. The product was purified by silica gel column chromatography with ethyl acetate/hexane (2:3) as the eluant, affording red-orange solids of bis-2-methylindolylmaleic acid anhydride (**7**) (1.5 g) in a 75% yield.

To a solution of **7** (1.0 g, 2.8 mmol) in THF were added aniline (0.52 mL, 5.7 mmol) and K_2CO_3 (200 mg). The mixture was heated to 60 °C for 24 h. It was allowed to cool to ambient temperature and was filtered. The product was purified by silica gel column chromatography with ethyl acetate/hexane/CH_2Cl_2 (1:3:2) as the eluant, affording dark red solids of bis-2-methylindolyl-*N*-phenylmaleimide (**8**) (1.1 g) in 91% yield. Physical data for **8**. Anal. Calcd for $C_{28}H_{21}N_3O_2$: C, 77.94; H, 4.91; N, 9.74. Found: C, 77.97; H, 4.70; N, 9.68. ^{1}H NMR (CD_3COCD_3, 400 MHz): δ 2.15 (s, 6H), 6.80 (t, 7 Hz, 2H), 6.98 (t, 7 Hz, 2H),7.22 (d, 8 Hz, 2H), 7.26 (d, 8 Hz, 2H), 7.37 (t, 7 Hz,1H), 7.51 (t, 7 Hz, 2H), 7.60 (d, 8 Hz, 2H), 10.41(s, 2H). ^{13}C NMR (CD_3COCD_3, 125 MHz, H-decoupled): δ 13.56, 104.97, 111.35, 120.31, 120.82, 122.00, 127.39, 127.73, 128.07, 129.41, 132.65, 134.19, 136.87, 138.46, 170.49. IR (KBr): 3409 (s), 3305 (s), 3061 (w), 2921 (w), 1756 (m), 1694 (s), 1606 (m), 1545 (m), 1457 (s), 1388 (s), 737 (s) cm^{-1}. MS (FAB): *m*/*e* 431 (M^+, 100%).

Compound **8** (800 mg, 1.86 mmol) was deprotonated with NaH (107 mg, 4.5 mmol) in THF (10 mL) under a nitrogen atmosphere, and the solution turned from red to blue in color. To the mixture was added iodomethane (0.28 mL, 4.5 mmol), and the solution turned to red immediately. The mixture was stirred with a magnetic bar at room temperature for 1 h. The reaction was quenched by the addition of water (500 mL), and the solution was filtered. The filtrate was recrystallized from CH_2Cl_2 and hexane to yield bright red crystalline solids of **1** (730 mg,85% yield). Physical data for **1**. Anal. Calcd for $C_{30}H_{25}N_3O_2$: C, 78.41; H, 5.48; N, 9.14. Found: C, 78.22; H, 5.34; N, 9.18. ^{1}H NMR ($CDCl_3$,500 MHz): δ 2.10 (s, 6H), 3.61 (s, 6H), 6.92 (br, 2H), 7.12 (t, 8 Hz, 2H), 7.21 (br, 2H), 7.23 (br, 2H), 7.36 (t, 8 Hz, 1H), 7.50 (t, 8 Hz, 2H), 7.57(d, 8 Hz, 2H). ^{13}C NMR ($CDCl_3$, 125 MHz, H-decoupled): δ 12.39, 29.79, 103.87, 108.78, 120.21, 121.46, 126.05, 127.16, 128.90,

(9) (a) Wang, Y.; Herron, N.; Grushin, V. V.; LeCloux, D.; Petrov, V. *Appl. Phys. Lett.* **2001**, *79* (4), 449−451. (b) Tsuzuki, T.; Shirasawa, N.; Suzuki, T.; Tokito, S. *Adv. Mater.* **2003**, *15*, 1455. (c) Gurge, R. M.; Sarker, A. M.; Lahti, P. M.; Hu, B.; Karasz, F. E. *Macromolecules* **1997**, *30* (26), 8286−8292.

131.42, 132.51, 137.21, 138.66, 170.49. IR (KBr): 3052 (w), 2923 (w), 1757 (m), 1701 (s), 1610 (m), 1534 (m), 1474 (m), 1387 (s), 736 (s) cm^{-1}. MS (FAB): *m*/*e* 459 (M^+, 100%).

2,3-Bis(2′,*N*-dimethyl-3′-indolyl)-*N*-pentafluorophenylmaleimide (1F). To a solution of 2-methylindole (2.0 g, 15 mmol) in toluene (200 mL) was added MeMgCl (3 M in THF, 5.1 mL) under a nitrogen atmosphere, and the solution was heated to 60 °C for 1 h. A solution of *N*-pentafluorophenyl-2,3-dichloromaleimide (1.00 g, 3.0 mmol) in toluene (15 mL) was then added, and the mixture was heated to reflux for 24 h. The solution turned from red to dark blue. It was allowed to cool to ambient temperature and was diluted by adding ethyl acetate (500 mL). The combined organic part was successively washed with HCl (1.0 N, 200 mL), water (200 mL), and brine (200 mL) and dehydrated over anhydrous $MgSO_4$. It was dried in vacuo, forming a dark red residue. The crude product was purified by silica gel column chromatography with ethyl acetate/hexane (1:4) as the eluant, affording bis(2-methylindolyl)-*N*-pentafluorophenylmaleimide (**8F**) (1.16 g, 74% yield). Physical data for **8F**. Anal. Calcd for $C_{28}H_{16}F_5N_3O_2$: C, 64.49; H, 3.09; N, 8.06. Found: C, 64.28; H, 3.27; N, 7.77. ^{1}H NMR (CD_3COCD_3, 400 MHz): δ 2.16 (s, 6H), 6.81 (t, 7.20 Hz, 2H), 7.00 (t, 7 Hz, 2H,), 7.16 (d, 8 Hz, 2H), 7.29 (d, 8 Hz, 2H), 10.59(s, 2H). ^{13}C NMR (CD_3COCD_3, 100 MHz, H-decoupled): δ 13.59, 104.60, 109.10, 111.57, 120.60, 122.27, 127.74, 133.29, 136.19, (137.8, 141.3) (d, 250 Hz, CF), 139.18, (141.3, 143.8) (d, 250 Hz, CF), (143.8, 146.3) (d, 250 Hz, CF), 168.57. ^{19}F NMR (CD_3COCD_3, 282 MHz): δ −143.92 (br, 2F, ortho), −154.23 (t, 21 Hz, 1F, para), −163.21 (t, 21 Hz, 2F, meta). IR (KBr): 3408 (s), 3332 (s), 3061 (w), 2925 (w), 1764 (m), 1707 (s), 1620 (m), 1603 (m), 1517 (s), 1458 (s), 739 (s) cm^{-1}. MS (FAB): *m*/*e* 521 (M^+, 100%).

Compound **8F** (1.00 g, 1.9 mmol) was dissolved in THF (10 mL) under a nitrogen atmosphere. NaH (110 mg, 4.6 mmol) was then added, and the mixture turned from red to dark blue. To the mixture was added iodomethane (0.36 mL, 5.8 mmol), and the solution turned red immediately. The mixture was stirred with a magnetic bar at room temperature for 1 h. The reaction was quenched by the addition of water (1.0 L), and the solution was filtered. The filtrate was recrystallized from CH_2Cl_2 and hexane to yield bright red crystalline solids of **1F** (970 mg, 92% yield). Physical data for **1F**. Anal. Calcd for $C_{30}H_{20}F_5N_3O_2$: C, 65.57; H, 3.67; N, 7.65. Found: C, 65.18; H, 3.77; N, 7.50. ^{1}H NMR (CD_2Cl_2, 400 MHz): δ 2.16 (s, 6H), 3.65 (s, 6H), 6.94 (t, 6.94 Hz, 2H), 7.14−7.18 (m, 4H), 7.29 (d, 8.10 Hz, 2H). ^{13}C NMR (CD_2Cl_2, 100 MHz, H-decoupled): δ 12.24, 29.89, 103.59, 108.20 (CF), 109.19, 119.95, 120.27, 121.65, 125.98, 132.57, (137.0, 139.5) (d, 250 Hz, CF), 137.36, (137.9, 140.5) (d, 250 Hz, CF), 139.45, (143.1, 145.6) (d, 250 Hz, CH), 168.11. ^{19}F NMR ($CDCl_3$, 282 MHz): δ −142.92 (m, 2F, ortho), −154.23 (t, 20 Hz, 1F, para), −163.21 (t, 21 Hz, 2F, meta). IR (KBr): 3051 (w), 2997 (w), 2940 (w), 1770 (m), 1721 (s), 1603 (m), 1521 (s), 1471 (m), 1437 (m), 1367 (m), 742 (s) cm^{-1}. MS (FAB): *m*/*e* 549 (M^+, 100%).

2,3-Bis(2′,*N*-dimethyl-3′-indolyl)-*N*-benzylmaleimide (2). Compound **6** (1.00 g, 2.8 mmol) was mixed with NaH (81 mg, 3.4 mmol) in DMF (10 mL) under a nitrogen atmosphere, and the solution turned gradually from red to dark blue. To the mixture was added benzyl bromide (0.40 mL, 2.3 equiv), and the solution turned red immediately. The mixture was stirred with a magnetic bar at room temperature for 1 h. The reaction was quenched by the addition of water (500 mL), and the solution was filtered. The filtrate was purified by silica gel column chromatography with ethyl acetate/hexane (1:3) as the eluant, affording 2,3-bis(2-methylindolyl)-*N*-benzylmaleimide (**9**) (460 mg, 40% yield) as red crystalline solids. Physical data for **9**. Anal. Calcd for $C_{29}H_{23}N_3O_2$: C, 78.18; H, 5.20; N, 9.43. Found: C, 78.17; H, 5.09; N, 9.43. ^{1}H NMR (CD_3COCD_3, 400 MHz): δ 2.09 (s, 6H), 4.84 (s, 2H), 6.77 (td, 2 & 8 Hz, 2H), 6.97 (td, 2 & 8 Hz, 2H), 7.12 (d, 8 Hz, 2H), 7.24 (dd, 2 and 8 Hz, 2H), 7.27 (m, 1H), 7.36 (t, 7 Hz, 2H), 7.45 (d, 7 Hz, 2H), 10.37 (s, 2H). ^{13}C NMR (CD_3COCD_3, 125 MHz, H-decoupled): δ 13.52, 42.15, 105.02, 111.33, 120.28, 120.70, 121.97, 128.01, 128.15, 128.70, 129.38, 132.59, 136.84, 138.26, 138.70, 171.88. IR (KBr): 3391 (s), 3339 (s), 3319 (s), 3060 (w), 3030 (w), 2942 (w), 2908 (s), 1755 (m), 1686 (s), 1619 (m), 1546 (m), 1457 (s),1399 (s), 747 (s) cm^{-1}. MS (FAB): *m*/*e* 445 (M^+, 100%).

Compound **9** (460 mg, 1.04 mmol) was treated again with NaH (60 mg, 2.5 mmol) in THF (10 mL) under a nitrogen atmosphere, andthe solution turned from red to blue. To the mixture was added iodomethane (0.28 mL, 4.5 mmol), and the solution turned red immediately. The mixture was stirred with a magnetic bar at room temperature for 1 h. The reaction was quenched by the addition of water (500 mL), and the solution was filtered. The filtrate was recrystallized from CH_2Cl_2 and hexane to yield bright red crystalline solids of **2** (410 mg, 83% yield). Physical data for **2**. Anal. Calcd for $C_{31}H_{27}N_3O_2$: C, 78.62; H, 5.75; N, 8.87. Found: C, 78.61; H, 5.68; N, 8.86. ^{1}H NMR ($CDCl_3$, 500 MHz): δ 2.02 (s, 6H), 3.58 (s, 6H), 4.88 (s, 2H), 6.92 (br, 2H), 7.11 (tm, 8 Hz, 4H), 7.25 (dm, 8 Hz, 2H), 7.33 (t, 7 Hz, 1H), 7.39 (t, 7 Hz, 2H), 7.51 (d, 8 Hz, 2H). ^{13}C NMR ($CDCl_3$, 125 MHz, H-decoupled): δ 12.27, 29.73, 41.86, 103.94, 108.70, 120.13, 120.19, 121.37, 125.94, 127.53, 128.59, 128.76, 131.47, 137.13, 138.35, 171.48. IR (KBr): 3046 (w), 2942 (w), 1752 (m), 1698 (s), 1619 (m), 1606 (m), 1536 (m), 1427 (s),1396 (s), 741 (s) cm^{-1}. MS (FAB): *m*/*e* 473 (M^+, 100%).

2,3-Bis(2′,*N*-dimethyl-3′-indolyl)-*N*-pentafluorobenzylmaleimide (2F). The preparation of **2F** was similar to that of **2**, starting from compound **6**. An intermediate compound **9F** was obtained in 63% yield. Physical data for **9F**. Anal. Calcd for $C_{29}H_{18}F_5N_3O_2$: C, 65.05; H, 3.39; N, 7.85. Found: C, 65.02; H, 3.21; N, 7.71. ^{1}H NMR (CD_3COCD_3, 400 MHz): δ 2.07 (s, 6H), 4.97 (s, 2H), 6.80 (t, 8 Hz, 2H), 6.97 (t, 7 Hz, 2H), 7.16 (d, 8 Hz, 2H), 7.22 (d, 8 Hz, 2H), 10.29 (s, 2H). ^{13}C NMR (CD_3COCD_3, 125 MHz, H-decoupled): δ 13.46, 29.80, 104.83, 111.36, 111.79 (CF), 120.36, 120.60, 122.03, 127.85, 132.51, 136.78, (137.3, 139.3) (d, 250 Hz, CF), 138.44, (140.5, 142.5) (d, 250 Hz, CF), (145.5, 147.5) (d, 250 Hz, CF), 171.08. ^{19}F NMR (CD_3COCD_3, 282 MHz): δ −142.83 (d, 23 Hz, 2F, ortho), −157.10 (t, 24 Hz, 1F, para), −164.26 (m, 2F, meta). IR (KBr): 3385 (s), 3058 (w), 2920 (w), 2853 (w), 1765 (m), 1705 (s), 1620 (m), 1507 (s), 1459 (m), 1400 (m), 742 (s) cm^{-1}. MS (FAB): *m*/*e* 535 (M^+, 100%).

The conversion of **9F** to **2F** was completed in 85% yield. Physical data for **2F**. Anal. Calcd for $C_{31}H_{22}F_5N_3O_2$: C, 66.07; H, 3.94; N, 7.46. Found: C, 66.28; H, 3.83; N, 7.48. ^{1}H NMR ($CDCl_3$, 400 MHz): δ 2.03 (s, 6H), 3.58 (s, 6H), 4.99 (s, 2H), 6.93 (br, 2H), 6.09−7.13 (m, 3H), 7.18−7.21 (m, 3H). ^{13}C NMR ($CDCl_3$, 100 MHz, H-decoupled): δ 12.28, 29.78, 30.00, 103.79, 108.78, 110.0 (t, 17 Hz, CF), 120.11, 120.32, 121.53, 125.91, 131.49, (136.2, 138.7) (d, 250 Hz, CF), 137.19, 138.57, (139.7, 142.3) (d, 250 Hz, CF), (144.3, 146.8) (d, 250 Hz, CF), 170.59. ^{19}F NMR ($CDCl_3$, 282 MHz): δ −142.8 (d, 22 Hz, 2F, ortho), −157.1 (t, 20 Hz, 1F, para), −163.3 (br, 2F, meta). IR (KBr): 3060 (w), 3007 (w), 2947 (w), 2908 (w), 1765 (m), 1706 (s), 1634 (m), 1613 (m), 1508 (s), 1474 (m), 1397 (m), 739 (s) cm^{-1}. MS (FAB): *m*/*e* 563 (M^+, 100%).

2,3-Bis(2′-methyl-*N*-benzyl-3′-indolyl)-*N*-benzylmaleimide (3). Compound **6** (3.0 g, 8.5 mmol) was mixed with NaH (650 mg, 27 mmol) in THF (35 mL) under a nitrogen atmosphere, and the solution turned from red to dark blue. To the mixture was added benzyl bromide (3.3 mL, 28 mmol), and the solution turned back to red again. The mixture was stirred with a magnetic bar at room

Scheme 1

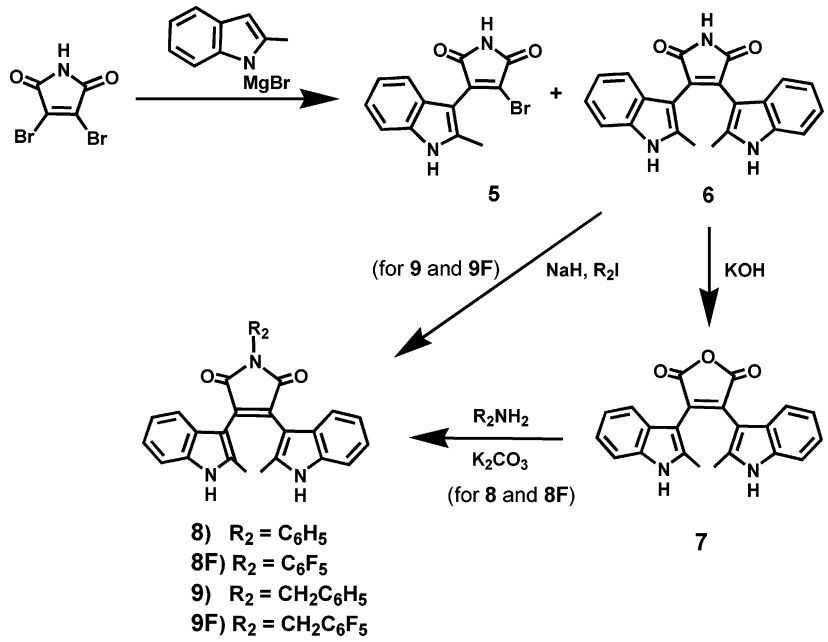

temperature for 8 h. The reaction was quenched by the addition of water (1.0 L), and the solution was filtered. The filtrate was recrystallized from CH_2Cl_2 and hexane to yield red crystalline solids of **3** (3.2 g, 61% yield). Physical data for **3**. Anal. Calcd for $C_{43}H_{35}N_3O_2$: C, 82.53; H, 5.64; N, 6.72. Found: C, 82.90; H, 5.67; N, 6.80. ^{1}H NMR ($CDCl_3$, 400 MHz): δ 2.03 (br, 6H), 4.89 (s, 2H), 5.25−5.30 (br, 4H), 6.71 (m, 3H), 6.93 (m, 3H), 7.00−7.24 (m, 13H), 7.26−7.32 (m, 1H), 7.35 (t, 7 Hz, 1H), 7.52(d, 7 Hz, 2H). ^{13}C NMR ($CDCl_3$, 100 MHz, H-decoupled): δ 12.30, 41.93, 46.59, 104.60, 109.25, 120.25, 120.45, 121.75, 125.72, 127.27, 127.58, 128.63, 128.72, 128.75, 131.91, 136.80, 136.93, 137.09, 138.05, 171.32. IR (KBr): 3031 (w), 2940 (w), 2910 (w), 1755 (m), 1695 (s), 1621 (m), 1607 (m), 1544 (m), 1518 (m), 1453 (m), 1428 (s), 1396 (s), 1353 (s), 737 (s) cm^{-1}. MS (FAB): *m*/*e* 626 (M^+, 93%).

2,3-Bis(2′-methyl-*N*-pentafluorobenzyl-3′-indolyl)-*N*-pentafluorobenzylmaleimide (3F). The procedure is similar to that of **3**, starting from **6** (1.5 g, 4.2 mmol) and pentafluorobenzyl bromide (2.3 mL, 15 mmol). The yield of **3F** was 66% (2.5 g). Physical data for **3F**. Anal. Calcd for $C_{43}H_{20}F_{15}N_3O_2$: C, 57.67; H, 2.25; N, 4.69. Found: C, 57.79; H, 2.21; N, 4.57. ^{1}H NMR ($CDCl_3$, 400 MHz): δ 1.99−2.26 (br, 6H), 4.99 (s, 2H), 5.20−5.32 (br, 4H), 6.84 (br, 2H), 6.97−7.17 (m, 6H). ^{13}C NMR ($CDCl_3$, 100 MHz, H-decoupled): δ 12.10, 30.04, 35.30, 105.18, 108.67, 109.92 (m, CF), 120.37, 120.63, 122.09, 125.27, 131.71, 136.38, (136.4, 138.8) (d, 240 Hz, CF), 138.15, (139.8, 142.4) (d, 260 Hz, CF), (143.8, 146.3) (d, 250 Hz, CF), (144.3, 146.8) (d, 250 Hz, CF), 170.11. ^{19}F NMR ($CDCl_3$, 282 MHz): δ −141.96 (d, 20 Hz, 4F, ortho of indoles), −142.24 (d, 21 Hz, 2F, ortho of maleimide), −153.38 (m, 2F, para of indoles), −154.68 (t, 20 Hz, 1F, para of maleimide), −161.22 (t, 20 Hz, 4F, meta of indoles), −162.07 (t, 21 Hz, 2F, meta of maleimide). IR (KBr): 3053 (w), 2959 (w), 2942 (w), 1765 (m), 1709 (s), 1620 (m), 1615 (m), 1524 (s), 1504 (s), 1460 (m), 1424 (m), 1399 (m), 739 (s) cm^{-1}. MS (FAB): *m*/*e* 895 (M^+, 100%).

2,3-Bis(*N*-methyl-2′-phenyl-3′-indolyl)-*N*-pentafluorophenylmaleimide (4F). A procedure similar to the preparation of **1F** was employed, except 2-phenylindole was used as a starting material instead of 2-methylindole. Physical data for **4F**. ^{1}H NMR ($CDCl_3$, 400 MHz): δ 3.50 (br, 6H), 6.66 (br, 2H), 6.90−7.40 (m, 16H). ^{13}C NMR ($CDCl_3$, 100 MHz, H-decoupled): δ 31.68, 104.66, 110.37, 119.65, 121.14, 123.08, 126.87, 128.48, 128.70, 130.45, 131.86, 133.73, (137.3, 139.8) (d, 250 Hz, CF), (140.8, 143.3) (d, 250 Hz, CF), 142.73, (143.3, 145.8) (d, 250 Hz, CF), 167.90. IR (KBr): 3048 (w), 2945, 1774 (m), 1721 (s), 1614 (m), 1524 (s), 1471 (m), 1358 (m), 1294 (m), 1100 (m), 1071 (m), 987 (m), 745 (m), 700 (m) cm^{-1}. MS (FAB): *m*/*e* 673 (M^+, 35%).

Results and Discussion

Synthesis. Most compounds (except **1F**) were prepared from bis-2-methylindolylmaleimide (**6**), which was made by a substitution reaction of dibromomaleimide with 2-methylindol-3-ylmagnesium bromide. A minor amount of monosubstituted derivative **5** was obtained even in the presence of a high molar ratio of the nucleophile. The product ratio of **6**:**5** also depended on reaction conditions, such as solvent polarity. Under suitable conditions, the yield of **6** could approach 90% regardless of the presence of **5**.

The *N*-alkylation processes for compound pairs **2**/**2F** and **3**/**3F** proceeded through the corresponding amides. A two-stage process was employed for the synthesis of **2** and **2F** in which the maleimide nitrogen was alkylated first, forming intermediates **9** and **9F**. Subsequent methylation of the indolyl nitrogens yielded the target products. A one-step reaction was employed for the preparation of compounds **3** and **3F** in which the three nitrogens of **6** were triply alkylated all at once.

The synthetic pathway for compounds **1** and **1F** was more complicated and is depicted in Scheme 1. The preparation of **1** started from maleimide **6**, which was first transformed to maleic anhydride **7** and then treated with aniline, yielding *N*-phenylmaleimide **8**. Subsequent deprotonation followed by *N*-methylation yielded **1**. Compound **1F** was prepared from commercially available 2,3-dichloro-*N*-pentafluorophenylmaleimide, which underwent substitution reactions with 2-methylindol-3-ylmagnesium bromide to yield **8F** in 74% yield. Methylation of **8F** to **1F** was completed in a way similar to that of **8**.

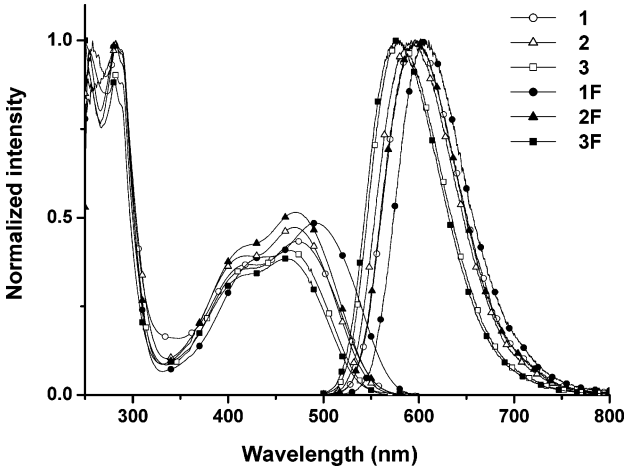

Figure 1. Absorption and emission spectra of compounds **1**−**3** and **1F**−**3F** in THF.

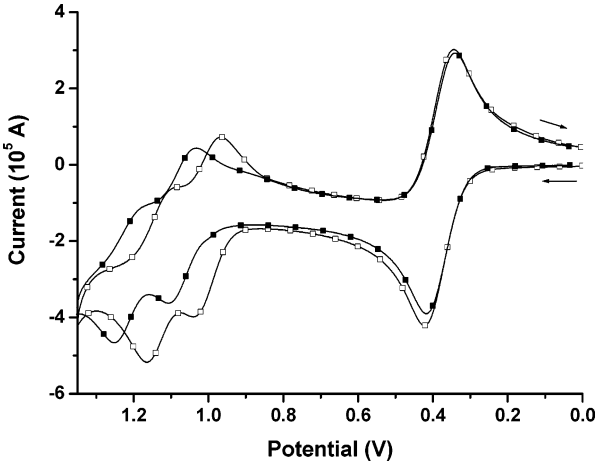

Figure 2. Oxidation potential of compounds **3** and **3F**, measured by cyclic voltammetry in acetonitrile. The redox waves at 0.35 V are derived from ferrocene, which was used as an internal standard.

All the above-mentioned compounds were collected as red crystalline solids and fully characterized by spectroscopic analyses. In their ^{1}H NMR spectra, line broadenings were observed at room temperature because of restricted rotation along C−C bonds connecting the indole and maleimide moieties. The methyl groups at C(2) of indoles prevent the two indole rings from being coplanar with the maleimide ring.

Physical Properties. *Absorption and Emission Spectra.* The absorption and emission spectra of **1**−**3** and **1F**−**3F** are shown in Figure 1. Two major absorption bands were observed in THF at λ_{max} 460−495 and 278−285 nm, with the former exhibiting a shoulder at 410−430 nm. These two bands were assigned to the $\pi-\pi^*$ transitions from the S_0 to S_1 and S_2 states, respectively, with a minor charge-transfer character that was discovered by De Cola and Williams et al.[10] However, a recent work published by Kosower pointed out that the long-wavelength absorption should come from an unusual $n_\pi \rightarrow \pi^*$ transition.[11] The transition happened by the transfer of an electron from the amide lone pair to a carbonyl π^*-orbital. The p-lobes in these orbitals are in a parallel alignment, resulting in a higher absorption intensity than that of the usual $n-\pi^*$ absorptions. The dipole moment of the ground-state molecules was not very high, because two cross-intercepted chromophores, from the indole nitrogen to the maleimide carbonyl, were present that passed each other along the central C═C bond. The two dipoles partially annul each other; therefore, the molecule exhibits a weak solvent effect in its absorption spectrum. For analogous monoindolylmaleimides, however, a much stronger dipole was found upon photoexcitation. As the asymmetric maleimides have only one dipole, there is no annulling of dipoles as there is in the symmetric compounds.[10b]

On irradiation at 475 nm, all compounds gave a red luminescence at λ_{em} 575−610 nm. The photoluminescence quantum yields of **1**/**1F**, **2**/**2F**, and **3**/**3F** in dioxane were estimated to be 0.23/0.11, 0.37/0.21, and 0.47/0.49, respectively. An explicit charge-transfer state is produced upon the $n_\pi \rightarrow \pi^*$ transition. The charge-transfer nature can be verified by the high sensitivity of the emission spectrum to the solvent polarity.[10,11] The amount of red shift observed in the emission spectra of **6** was found to be substantially greater than that of the corresponding monosubstituted homologues such as **5**.

The fluorine-substituent effect was not apparent upon examination of the spectra in Figure 1. A mild red shift was observed for **1F** in both the absorption and emission spectra compared to those of **1**. For compound pairs **2**/**2F** and **3**/**3F**, the spectral shift are less apparent; as in the benzyl substituents, the pentafluorophenyl group was not conjugated with the amide nitrogen.

Redox Potentials. The oxidation potentials were measured by cyclic voltammetry (CV) in acetonitrile. Each compound showed two consecutive anodic peaks separated by ca. 120 mV in the oxidative sweep, which correspond to the oxidation of the two indolyl moieties (Figure 2). The oxidative potentials for the fluorinated derivatives (**1F**−**3F**) were slightly higher than those of the parent compounds (**1**−**3**), whereas the reductive potentials of the former were lower than those of the latter (Table 1). A single reductive wave was observed for each compound in the range −1.1 to −1.3 V (Figure 3). The band gaps, estimated by the difference between E_{ox} and E_{red}, were the energy difference between the highest occupied molecular orbital (HOMO) and the lowest unoccupied molecular orbital (LUMO). These values can also be estimated by the 0−0 absorption energies in their UV spectra, which were estimated from the interception of the absorption and emission spectra. The HOMO−LUMO gaps measured by both methods were found to be consistent with each other, as shown in Table 1.

The reversibility of the redox waves indicated a high electrochemical stability of these compounds. The bandwidth between the cathodic and anodic peaks was estimated to be about 73 mV. The differences between nonfluorinated (**1**−

(10) (a) Zerbetto, F.; De Cola, L.; König, B.; Williams, R. M. *J. Phys. Chem. A* **2005**, *109*, 6440−6449. (b) Kaletas, B. K.; Joshi, H. C.; van der Zwan, G.; Fanti, M.; Zerbetto, F.; Goubitz, K.; De Cola, L.; König, B.; Williams, R. M. *J. Phys. Chem. A* **2005**, *109*, 9443−9455.

(11) (a) Kosower, E. M.; de Souza, J. R. *Chem. Phys.* **2005**, accepted. (b) ter Steege, D. H. A.; Buma, W. J. *J. Chem. Phys.* **2003**, *118* (24), 10944−10955. (c) Climent, T.; González-Luque, R.; Merchán, M. *J. Phys. Chem. A* **2003**, *107*, 6995−7003. (d) Peng, Q.; Lu, Z.; Huang, Y.; Xie, M.; Xiao, D.; Zou, D. *J. Mater. Chem.* **2003**, *13*, 1570−1574.

Table 1. Absorption Energy, Oxidation, and Reductive Potentials of Compounds 1−3 and 1F−4F

	λ_{max} (ϵ)[a] (nm)	Φ[b]	λ_{0-0}[c] (nm)	E_{0-0} (eV)	E_{ox}[d] (V)	E_{red}[d] (V)	band gap[e] (eV)	HOMO[f] (eV)	LUMO[g] (eV)
1	475 (6700)	0.23	538	2.30	0.88, 1.02	−1.34	2.22	−5.28	−3.06
1F	495 (8400)	0.11	555	2.23	0.92, 1.07	−1.19	2.11	−5.32	−3.21
2	470 (6800)	0.37	535	2.32	0.87, 0.99	−1.38	2.45	−5.27	−3.02
2F	471 (8200)	0.21	538	2.30	0.98, 1.10	−1.34	2.31	−5.38	−3.06
3	465 (6900)	0.47	526	2.36	0.98, 1.10	−1.34	2.31	−5.38	−3.07
3F	462 (7400)	0.49	522	2.38	1.06, 1.20	−1.26	2.32	−5.46	−3.14
4F	490 (8300)	0.27	575	2.16	0.96, 1.23	−1.12	2.08	−5.36	−3.28

[a] Extinction coefficient in dioxane. [b] Quantum yield in dioxane (see ref 12a). [c] Taken at the crossing point of the absorption and emission spectra. [d] Fc/Fc^+ at 0.35 V against $Ag/AgNO_3$ as the internal reference. [e] Gap between E_{ox} and E_{red}. [f] Calculated as $-(E_{ox} + 4.40)$ (see ref 12b,c). [g] Calculated as HOMO + band gap.

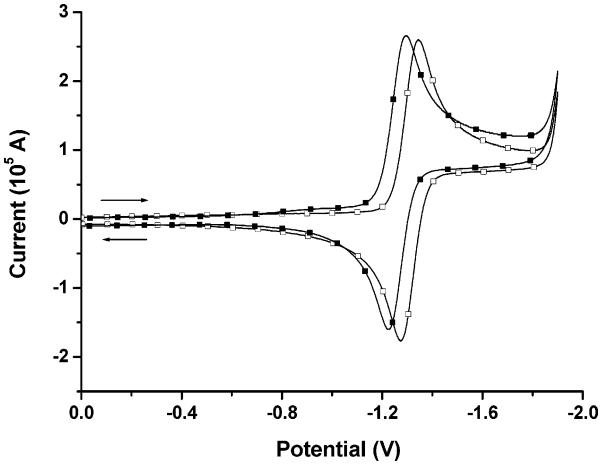

Figure 3. Reductive potential of compounds **3** and **3F**, measured by cyclic voltammetry in acetonitrile.

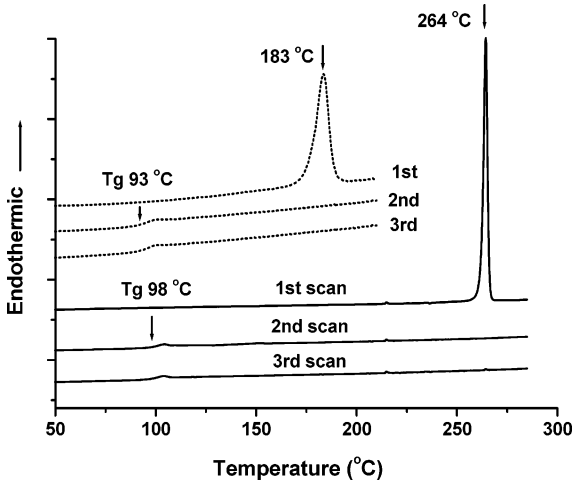

Figure 4. DSC plots of compounds **3** (solid lines) and **3F** (dotted lines). The samples were heated at 20 °C/min during the first scan and then cooled at the same rate. The process was repeated, with the second and third scans showing a similar pattern. Glass-transition temperatures (T_g) appeared at 98 and 93 °C (onset) for **3** and **3F**, respectively, with corresponding melting temperatures (T_m) at 264 and 183 °C (peak maximum), respectively.

Table 2. Glass-Transition Temperatures (T_g) and Melting Temperatures (T_m) of Compounds 1−3 and 1F−4F[a]

	1	**1F**	**2**	**2F**	**3**	**3F**	**4F**
T_g (°C)[b]	126	114	101	99	98	93	126
T_m (°C)[c]	276	287	233	226	264	183	284

[a] Estimated by differential scanning calorimetry (DSC). [b] Onset of peaks. [c] Peak maxima.

3) and fluorinated (**1F**−**3F**) derivatives, however, were only marginal.

Film Morphology. It has been shown by single-crystal diffraction analyses on certain derivatives that the two indole groups are not aligned coplanar to the maleimide ring.[2] Hindered rotation along the single bonds connecting the two moieties induced a line broadening in ^1H NMR spectra even at ambient temperature. There exist two conformational isomers according to the orientation of the indolyl substituents, i.e., a pseudo-*E* form and a pseudo-*Z* form. A polymorphous state has been detected by differential scanning calorimetry (DSC) for the existence of more than one type of crystalline geometry. The formation of amorphous film was believed to be responsible for the high intensity of red luminescence in the solid state.

Amorphous glass is in a thermodynamically nonequilibrium state, which usually exhibits a glass-transition phenomenon. A typical graph of DSC for compounds **3** and **3F** is shown in Figure 4. For compound **3**, the compound was heated at a rate of 20 °C/min. An endothermic peak appeared at 264 °C, which corresponds to the melting point (T_m) of the crystals. After a slow cooling process (at 20 °C/min), the same sample was heated again. In the second run, a small endothermic hump was detected at 98 °C, which was assigned to a glass-transition temperature (T_g). This signal then persists on repeated scans. The presence of T_g indicated the existence of an amorphous state of these molecular materials. The behavior of **3F** was similar to that of **3**, where T_g was found to be 93 °C and T_m 183 °C. Glass-transition phenomena were observed for all six compounds, and their T_g values are listed in Table 2. Amorphous films were likely to be formed upon vapor deposition during device fabrications. The high thermal stability was confirmed by TGA experiments. No sign of decomposition appeared upon heating below 350 °C.

The differences between fluorinated and nonfluorinated analogues were not significant. Compounds **1F**−**3F** showed T_g values slightly lower than those of **1**−**3**, whereas their T_m values did not exhibit any clear trend.

LED Devices. Two standard types of devices were made with configurations of ITO/NPB/maleimide/AlQ_3/Mg:Ag (device A) and ITO/NPB/maleimide/TPBI/Mg:Ag (device B). In these devices, NPB worked as a hole transporter (HT), while either AlQ_3 or TPBI was used as an electron transporter (ET). Both kinds of devices were prepared by fluorinated (**1F**−**4F**) and nonfluorinated compounds (**1**−**3**) for comparison purposes. Energy-level diagrams of devices A and B are shown in Figure 5. The only difference between the two kinds of devices was the ET materials, i.e., AlQ_3 and TPBI, which possess different HOMO and LUMO levels. The HOMO level of AlQ_3 (5.7 V) is substantially higher than that of TPBI (6.2 V). In device B, a higher energy

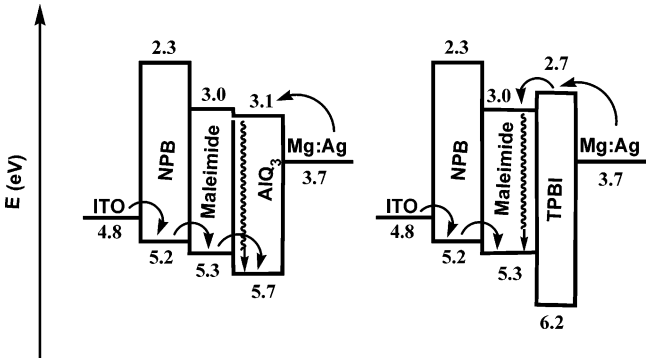

Figure 5. Relative energy levels in double heterojunction devices A (left) and B (right). In device A, holes moved readily into the bulk of AlQ_3 and recombined with electrons in both layers of maleimide and AlQ_3. In device B, TPBI acted as a hole blocker, so the charge recombination happened mostly in the maleimide layer.

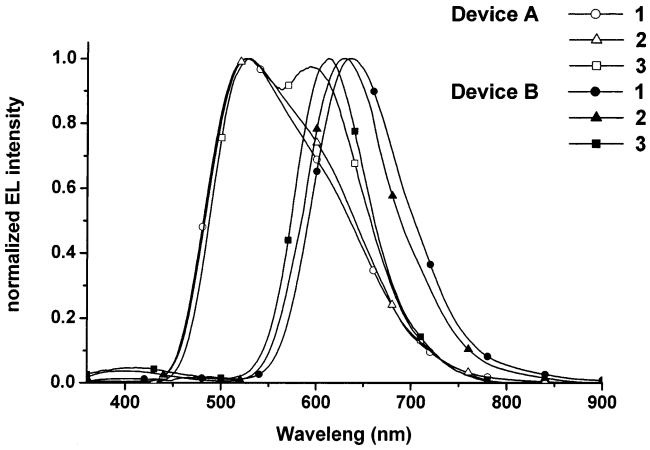

Figure 6. Electroluminescence of compounds **1** (○, ●), **2** (△, ▲), and **3** (□, ■) in two kinds of devices (A and B). The emissions centered at 630−660 nm are derived from maleimides **1**−**3**, whereas those centered at 520 nm are from AlQ_3. The minor bands at ca. 400 nm come from TPBI.

barrier retards the migration of holes across the film boundary between maleimide (ca. 5.3 V) and TPBI.[13]

The visual color electroluminescence (EL) of device A, fabricated by using both fluorinated and nonfluorinated maleimide dyes, was essentially yellow. Two emission maxima appeared in their spectra (Figure 6), i.e., the emission of AlQ_3 at λ_{max} 520 nm and that of maleimides at ca. 600 nm. The dual emission indicated that charge recombinations proceeded simultaneously in both layers of AlQ_3 and maleimide. Replacing the layer of AlQ_3 by TPBI hindered the migration of holes into the layer of TPBI. A pure red color emission was obtained in device B using nonfluorinated compounds **1**−**3** (Figure 6) as the emitter. In these devices, the emission intensity of TPBI at ca. 400 nm became negligibly low.

The situation was different when the emitting materials in device B were replaced by the fluorinated maleimides, i.e., **1F**−**4F**. A high-energy band appeared at λ_{max} 410 nm

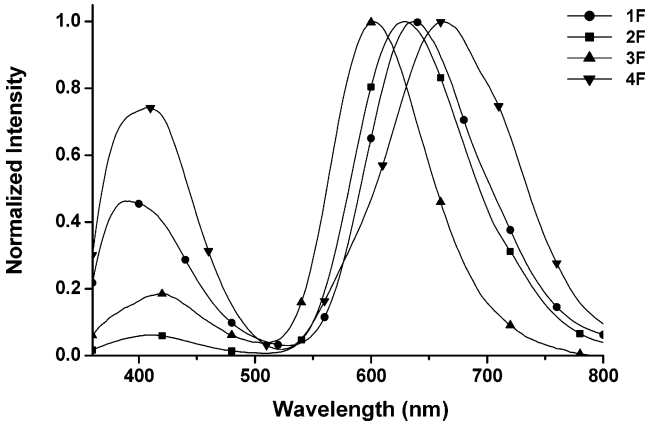

Figure 7. Electroluminescence of device B using maleimide dyes **1F** (●), **2F** (■), **3F** (▲), and **4F** (▼). All devices exhibited dual emissions coming from the TPBI (ca. 400 nm) as well as maleimide (600∼660 nm) layers. The former resulted from charge recombination by the holes, which leaked into the TPBI layer.

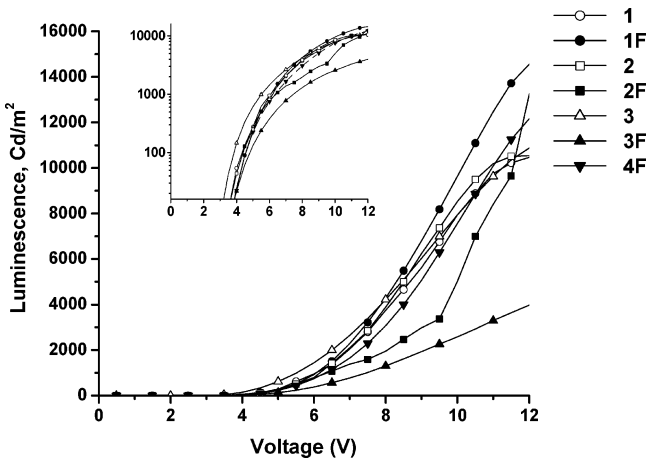

Figure 8. Intensity (*L*) vs voltage (*V*) plots of device A using the seven maleimide dyes. The inset shows the plots of log(*L*) vs *V*, in which the turn-on voltages can be readily identified.

with significant intensity, which corresponds to the emission of TPBI (Figure 7). In these devices, the migration of holes was not completely blocked from the TPBI layer. The presence of fluorine atoms has played a role in enhancing the efficiency of holes passing through the film boundary.

There are two possible explanations for this phenomenon. The first is that the presence of pentafluorophenyl substituents has changed the morphology of solid films. The low surface potential of fluorine atoms may have influenced the intermolecular interactions, thus changing the macroscopic appearance of the films and facilitating a better medium for hole transportation. The second explanation may rely on the high electronegativity of pentafluorophenyl groups. The strong electron-withdrawing nature of fluorine substituents may have lowered the potential levels of both HOMO and LUMO, therefore reducing the energy gap between maleimides and TPBI. It may be worth noting that in some structures (e.g., **2F** and **3F**), the pentafluorobenzyl groups are not conjugated with the major π-chromophores.

As indicated by DSC analyses, all compounds formed amorphous glasses with observable T_g values upon heating (Table 2). No clear distinction was found between the fluorinated and nonfluorinated compounds. The results of CV, however, confirmed that the oxidation potentials of

(12) (a) Morris, J. V.; Mahaney, M. A.; Huber, J. R. *J. Phys. Chem.* **1976**, *80*, 969. (b) Pommerehne, J.; Vestweber, H.; Guss, W.; Mahrt, R. F.; Bässler, H.; Porsch, M.; Daub, J. *Adv. Mater.* **1995**, *7*, 551. (c) Janietz, S.; Bradley, D. D. C.; Grell, M.; Giebeler, C.; Indasekaran, M.; Woo, E. P. *Appl. Phys. Lett.* **1998**, *73*, 2453.

(13) (a) Koene, B. E.; Loy, D. E.; Thompson, M. E. *Chem. Mater.* **1998**, *10*, 2235. (b) Tao, Y.-T.; Balasubramaniam, E.; Danel, A.; Tomasik, P. *Appl. Phys. Lett.* **2000**, *77*, 933. (c) Balasubramaniam, E.; Tao, Y.-T.; Danel, A.; Tomasik, P. *Chem. Mater.* **2000**, *12*, 2788.

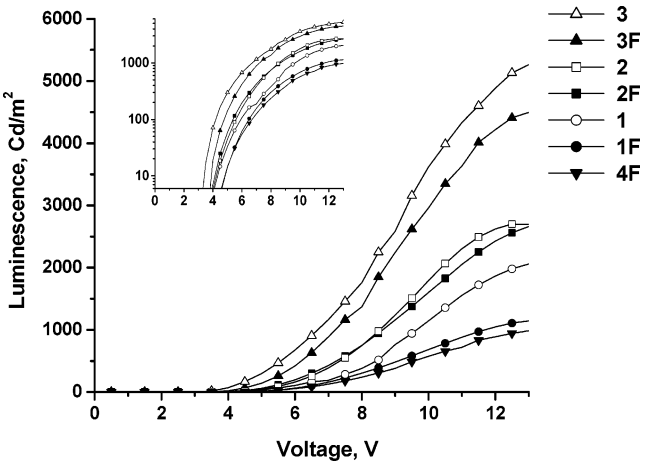

Figure 9. Intensity (L) vs voltage (V) plots of device B using the seven maleimide dyes. The inset shows the plots of log(L) vs V, in which the turn-on voltages can be readily identified.

Table 3. Performance of Devices A (ITO/NPB/maleimide/AlQ_3/Mg:Ag) and B (ITO/NPB/maleimide/TPBI/Mg:Ag) Using Maleimides 1−3 and 1F−4F as Emitting Materials

	turn-on	luminance (Cd/m^2)		max. Φ	
	(V)	100 mA/cm^2	max.	(%)	CIE coordinates[a]
			Device A		
1	4.0	1170	10 400 at 12 V	0.42	526 (0.38, 0.50)
1F	3.7	1930	14 800 at 12 V	0.76	522 (0.33, 0.54)
2	3.7	1180	10 500 at 12 V	0.39	526 (0.39, 0.50)
2F	3.7	1960	16 800 at 14 V	0.71	530 (0.39, 0.52)
3	3.3	1620	11 400 at 13 V	0.63	530 (0.42, 0.50)
3F	4.0	1100	6800 at 13 V	0.40	600 (0.50, 0.45)
4F	3.0	1800	13 000 at 13V	0.57	520 (0.33, 0.54)
			Device B		
1	4.1	240	2710 at 13 V	0.34	636 (0.63, 0.36)
1F	4.6	200	2780 at 14 V	0.45	638 (0.50, 0.28)
2	4.1	390	2700 at 14 V	0.32	630 (0.61, 0.37)
2F	3.9	460	2800 at 14 V	0.38	630 (0.60, 0.37)
3	3.4	980	5400 at 14 V	0.55	612 (0.58, 0.39)
3F	3.8	800	4600 at 14 V	0.50	602 (0.52, 0.38)
4F	4.0	130	1030 at 14 V	0.25	662 (0.42, 0.23)

[a] Commission Internationale de I'Eclairage 1931.

fluorinated derivatives were noticeably lower than those of the nonfluorinated ones. A lower oxidation potential means a lower potential energy for the HOMO (Table 1). Therefore, the energy barrier was reduced, allowing holes to migrate more easily across the film boundary into TPBI (Figure 5).

The performance of both devices A and B can be depicted by intensity vs voltage plots shown in Figures 8 and 9. All devices can be turned on at about 4 V. The intensity of device A was generally higher than that of device B (Table 3). The quantum efficiencies of both devices were similar, however, within a range of ca. 0.2−0.5% (Figure 10). From the plots shown in Figures 8−10, it appears that the performances of the devices made of fluorinated and nonfluorinated materials were not much different from each other.

The dual emission from separated layers in the devices made of fluorinated materials may be used as an advantage for tuning the color of devices.[14] It provides an alternative

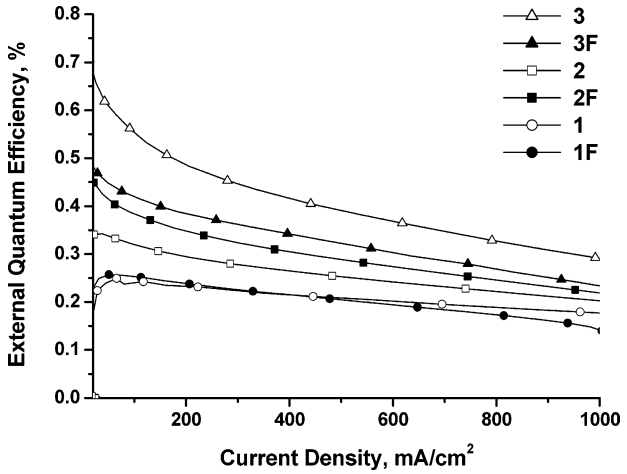

Figure 10. Plots of external quantum efficiency vs current density for device B.

method to the usual way of mixing two colored dopants together in a common matrix. Energy transfers happen inevitably when two chromophores are located too close to each other, which happens commonly among mixed dopants. Such a potential defect may be avoided in a design in which the two emitting species are separated. The visual color of such a device can be changed properly by adjusting the relative intensity of each emitting layer. Using maleimides as a red emitter, we may fabricate devices of various colors by combining the maleimide with another emitter in a multilayer design.

Summary

Bisindolylmaleimide derivatives **1**−**3** and their fluorinated analogues **1F**−**4F** were prepared and applied successfully to the fabrication of LED devices. All compounds form amorphous glasses in solid-state films. For fluorinated materials, red emissions can be obtained by the devices in an ITO/NPB/**1**−**3**/TPBI/Mg:Ag configuration (device B), whereas dual emissions were observed on the devices using AlQ_3 as the ET material (device A). For fluorinated materials, dual emissions were observed on both types of devices. The second emission came from either AlQ_3 or TPBI as a result of holes that migrated across the interface between maleimide and ET. Compounds containing pentafluorophenyl moieties exhibited reduced potential energy in both HOMO and LUMO levels, thus lowering the energy barrier for the movement of holes (Figure 5). Other than this difference, the general performances of fluorinated and nonfluorinated materials were quite similar to each other.

Acknowledgment. Financial support from Academia Sinica and the National Science Council of the Republic of China is gratefully acknowledged.

CM052198Y

(14) Chow, T. J.; Tsai, S.-H.; Chiu, C.-W.; Yeh, T.-S. *Synth. Met.* **2005**, *149*, 59.